THE JOURNAL OF PHYSICAL CHEMISTRY C

Article

pubs.acs.org/JPCC

Ab Initio Electronic Gaps of Ge Nanodots: The Role of Self-Energy Effects

Margherita Marsili,*[,†] Silvana Botti,[‡,¶,#] Maurizia Palummo,[§,#] Elena Degoli,[∥,#] Olivia Pulci,[§,#] Hans-Christian Weissker,[⊥,#] Miguel A. L. Marques,[¶,#] Stefano Ossicini,[∥,#] and Rodolfo Del Sole[§,#]

[†]Dipartimento di Fisica e Astronomia "Galileo Galilei", Universitá di Padova, via Marzolo 8, I-35131 Padova, Italy

[‡]Laboratoire des Solides Irradiés, École Polytechnique, CNRS, CEA-DSM, 91128 Palaiseau, France

[¶]Institut Lumière Matière, UMR5306 Universitè de Lyon 1-CNRS, Universitè de Lyon, F-69622 Villeurbanne, Cedex, France

[§]NAST and Dipartimento di Fisica, Università di Roma "Tor Vergata", Via della Ricerca Scientifica 1, I-00133 Rome, Italy

[∥]Istituto Nanoscienze CNR and Dipartimento di Scienze e Metodi dell'Ingegneria, Universitá di Modena e Reggio Emilia, I-42122 Reggio Emilia, Italy

[⊥]Aix-Marseille University, CNRS, CINaM UMR 7325, 13288 Marseille, France

[#]European Theoretical Spectroscopy Facility (ETSF)

ABSTRACT: Nanostructuring of a material leads to enormous effects on its excited state properties. This study, through the application of different state-of-the-art ab initio theoretical tools, investigates the effect of size on the electronic gap of germanium nanocrystals highlighting similarities and differences with respect to equivalent silicon nanostructures. We performed both GW and ΔSCF calculations for the determination of their electronic structure. While it is known that ΔSCF corrections to the Kohn−Sham gap vanish for extended systems, the two approaches were expected to be equivalent in the limit of small clusters. However, it has been recently found that for hydrogenated Si clusters the ΔSCF gaps are systematically smaller than the GW ones, while the opposite is true for Ag clusters. In this work we find that the GW gaps are larger than the ΔSCF ones for all the Ge dots, with the exception of the smallest one. Such crossing between the ΔSCF and the GW gap values was not expected and has never been observed before. Moreover, also for hydrogenated Si nanocrystals we found a similar behavior. The origin of this crossing might be found in the Rydberg character of the LUMO of the smallest clusters and can also explain the qualitative differences in the comparison between GW and ΔSCF found in the previous studies.

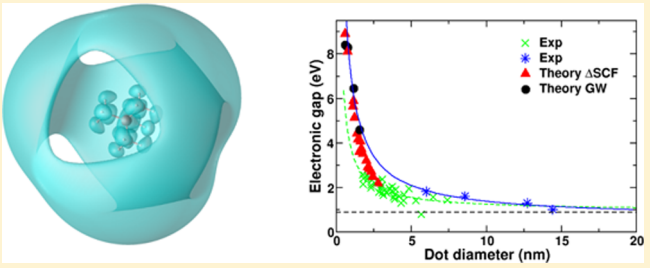

INTRODUCTION

The possibility of tailoring the electronic and optical properties of nanostructures simply by changing their size opens the way for the application of these systems in a variety of different fields, ranging from opto-electronics to photovoltaic devices. Many different materials, such as Si, CdTe, and III−V materials have seen their electronic gap engineered through the control of the size of the structures they constituted. Empirical or ab initio calculations, at the level of density functional theory (DFT), are able to capture qualitatively this effect. Nonetheless, to describe it in a more accurate way, it has often been necessary to go beyond standard ground state DFT calculations, using the so-called ΔSCF method within the DFT framework,[1] or the more sophisticated, but computationally demanding, GW approximation within the many-body perturbation theory (MBPT) framework.[2,3] For a long time the two theoretical approaches have been considered almost equivalent in the limit of small cluster diameters. However, recent studies on Si[4] and Ag clusters[5] have shown that the two methods are not equivalent. Moreover the discrepancy between the two methods is qualitatively different for the two systems: the ΔSCF gaps are larger than the GW ones in the Ag clusters case, while, on the contrary, in Si clusters the ΔSCF gaps are smaller than the GW ones.

Recent scanning-tunneling spectroscopy (STS) experiments[6,7] have measured the strong dependence of the electronic gap of Ge nanodots on their size. As expected, quantum-confinement effects lead to a strong increase of the gap when the dot diameter was reduced. Despite the simplicity of these systems and the analogy with their, more extensively studied, Si counterparts, only ΔSCF calculations of their electronic gap have been reported.[8] On Ge, no systematic investigation of their electronic gap within the MBPT framework has been carried out yet.

In this work, we present calculations of quasiparticle gaps for hydrogenated Ge nanocrystals of increasing size, with diameters ranging from 0.6 to 1.6 nm, using both ΔSCF-LDA and the perturbative GW method.

Received: December 10, 2012
Revised: June 10, 2013

   dx.doi.org/10.1021/jp3121269 | J. Phys. Chem. C XXXX, XXX, XXX−XXX

Our results show that, already for small clusters, the discrepancy between the two methods cannot be neglected, in agreement with previous results on Si[4] and Ag clusters.[5] However, neither the Si, nor the Ag clusters scenario is found in our case: while the GW gaps of the larger dots exceed the ΔSCF value (as in Si clusters), the value of the GW gap of the smallest Ge dot under investigation is smaller than the ΔSCF (as in Ag clusters). This peculiar crossing between the results of the two approaches required further investigation: we thus extended our study to the review of the Si dots case, finding a similar trend. As will be discussed below, the Rydberg character of the lowest empty state is responsible for this result.

Theoretical Background and Computational Details. The DFT Kohn−Sham method, while providing an excellent description of the ground state properties of materials, yields strongly underestimated electronic band gaps. The DFT KS gap E_g^{KS} of the N particle system, defined as the energy difference between the lowest unoccupied Kohn−Sham orbital (LUMO) and the highest occupied Kohn−Sham orbital (HOMO), is related to the quasiparticle gap, as measured by direct and inverse photoemission or by STS, through the discontinuity δ of the exchange and correlation (xc) potential when an electron is added to the system:

$$E_g = E_g^{KS} + \delta = \varepsilon_{N+1}^{(N)} - \varepsilon_N^{(N)} + v_{xc}^{+} - v_{xc}^{-} \quad (1)$$

where $\varepsilon_{N+1}^{(N)}$ ($\varepsilon_N^{(N)}$) is the lowest unoccupied (highest occupied) Kohn−Sham eigenvalue of the N-particle ground state DFT calculation. Since the discontinuity of the xc potential gives a substantial contribution[9,10] in eq 1, an accurate evaluation of the quasiparticle gap requires either to go beyond a single ground state calculation for the N electron system, or to move from the standard Kohn−Sham formalism to a so-called generalized Kohn−Sham scheme that employs nonlocal xc potentials.[11,12]

It is still possible to address the issue of the fundamental gap within the DFT framework if one starts from its definition in terms of electron affinity EA and ionization potential IP. This definition gives the fundamental gap in terms of the ground state total energy (E^{tot}) of N, $(N + 1)$, and $(N - 1)$-electron systems:

$$E_g = IP - EA = E_{N+1}^{tot} + E_{N-1}^{tot} - 2E_N^{tot} \quad (2)$$

As a result, within this so-called ΔSCF scheme, the determination of the fundamental electronic gap is in principle achieved at the computational cost of three DFT ground state calculations.[1] However, as the xc potential is unknown in its exact form, the application of this theory relies on approximations for the xc functional (such as LDA, GGA, etc.): we will refer to the use of the LDA functional within a ΔSCF calculation as ΔSCF-LDA.

The Green's function formalism provides a legitimate way to access the single-particle excitation energies, which appear as the poles of single-particle Green's functions. Within this scheme, it can be shown that quasiparticle energies are the solution of a single-particle equation in which the quasielectrons experience the external ($V_{ext}(\mathbf{r})$) and Hartree ($V_H(\mathbf{r})$) potentials, and a nonlocal, non-Hermitian, energy-dependent potential given by the electronic self-energy $\Sigma(\mathbf{r},\mathbf{r}', \omega)$.[2]

Neglecting vertex corrections, Σ is approximated by the product of the single-particle Green's function (G) and the screened Coulomb interaction (W), namely Σ = iGW. The GW approximation for the self-energy is the state-of-the-art theoretical tool for the calculation of band-structures and electronic properties of materials, surfaces, and nanostructures. However, its application to large systems is often limited by the computational effort that it requires.

It is useful, following ref 13, to identify the missing contribution to the band gaps of the KS scheme as $\delta\Sigma$, and the one of Δ$SCF-LDA as Δ, namely:

$$E_g = E_g^{KS} + \delta\Sigma = E_g^{\Delta SCF} + \Delta \quad (3)$$

For extended systems the use of continuous (with respect to the particle number) xc potentials like the LDA one in eq 2 leads to ΔSCF gaps equal to the Kohn−Sham gaps (i.e., strongly underestimated), so for bulks we have that $\Delta_b = \delta\Sigma_b$. Concerning confined systems, it was argued in ref 13 that the surface self-energy contribution, which is a macroscopic surface polarization term, can be well described by solving eq 2 within LDA. Moreover, assuming that the exchange contribution to the gap correction for the finite systems is the same as in the bulk, it was shown in ref 13 that the only correction that is missing to the ΔSCF results in the case of 0-D systems is given by the bulk self-energy term (~0.5 eV for Ge).

Computational Details. All ground state geometries were obtained with the use of the PWSCF code,[14] using norm-conserving LDA exchange-correlation pseudopotentials, and an energy cutoff for the plane-wave expansion of the wave functions of 30 Ryd. The Ge pseudopotentials included nonlinear core corrections. The supercell used for each calculation is reported in Table 1. Spin−orbit coupling corrections to the DFT HOMO−LUMO gap in hydrogenated Ge clusters of similar sizes are less than 0.1 eV,[15] therefore spin−orbit coupling has not been included in our calculations.

Table 1. Calculation Parameter for the DFT Ground State and GW Calculations

dot	supercell	lattice parameter (bohr)	bands χ_0	$N_G\,\chi_0$	$N_G\,\Sigma_x$
Ge_5H_{12}	cubic	40	500	4000	30000
$Ge_{10}H_{16}$	cubic	30	550	3000	5000
$Ge_{35}H_{36}$	cubic	50	900	4000	16000
$Ge_{87}H_{76}$	cubic	60	1000	6400	98745
Si_5H_{12}	cubic	40	500	1500	30000
$Si_{10}H_{16}$	cubic	50	530	10000	10000
$Si_{35}H_{36}$	cubic	40	1000	10000	20000
$Si_{87}H_{76}$	cubic	60	1000	15000	40000

The GW calculations on the Ge dots have been performed with use of the Yambo-code.[16] All the calculation parameters have been carefully converged until the electronic gap changed less than 0.1 eV. The calculation parameters such as the bands included in the calculation of the RPA dielectric matrix (bands χ_0), the dimension in terms of G-vectors of the RPA dielectric matrix ($N_G\,\chi_0$), and the number of G-vectors in the calculation of the exchange part of the self-energy ($N_G\,\Sigma_x$), are listed in Table 1. We have employed a spherical cutoff of the Coulomb potential in order to avoid the spurious interaction between dots belonging to neighboring supercells and to speed up the convergence of the GW calculation with respect to the supercell size.[17]

The ΔSCF calculations were performed with use of the code octopus.[18] The LDA[19] is employed in the adiabatic approximation for the xc potential and the electron-ion interaction is described through the same norm-conserving

dx.doi.org/10.1021/jp3121269 | J. Phys. Chem. C XXXX, XXX, XXX−XXX

pseudopotentials[20] used for GW calculations. The Kohn−Sham equations are represented in octopus in a real-space regular grid, for which we used a spacing of 0.275 Å that guarantees the convergence of all calculations. The simulation box is constructed by joining spheres centered around each atom, whose radius goes from 0.65 to 1.55 nm depending on the size and the charge of the cluster.

RESULTS

We have studied tetrahedrally coordinated Ge nanoparticles of increasing diameter (from 0.6 to 1.6 nm). The dangling bonds of the surface Ge atoms have been saturated by hydrogen, and the structures fully relaxed to their ground state[14] within DFT-LDA. The resulting geometries of the three larger Ge clusters are shown in Figure 1. A test calculation including the spin

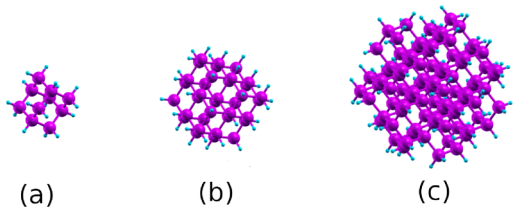

Figure 1. Ground state geometries of three of the Ge clusters under study: (a) $Ge_{10}H_{16}$ d = 0.7 nm, (b) $Ge_{35}H_{36}$ d = 1.4 nm, and (c) $Ge_{87}H_{76}$ d = 1.7 nm.

degrees of freedom within the local-spin density approximation (LSDA) revealed that the ground state of these systems is nonmagnetic. Starting from the same relaxed geometries we have performed both GW[16] and ΔSCF-LDA calculations.[18] The results of the calculations are listed in Table 2. A

Table 2. Quasiparticle Gaps Calculated within the ΔSCF-LDA and the GW Methods for Ge Clusters of Increasing Diameter

dot	diameter (nm)	DFT (eV)	ΔSCF-LDA (eV)	GW (eV)	GW-(ΔSCF-LDA) (eV)	GW-DFT (eV)
Ge_5H_{12}	0.60	5.7	8.9	8.4	−0.5	2.7
$Ge_{10}H_{16}$	0.76	4.8	8.1	8.3	0.2	3.5
$Ge_{35}H_{36}$	1.15	3.5	5.9	6.5	0.6	3.0
$Ge_{87}H_{76}$	1.56	2.5	3.6	4.6	1.0	2.1

qualitative description of the quantum size effects can already be obtained at the LDA Kohn−Sham level, as can be seen from Table 2: the Kohn−Sham gap increases from 2.5 to 5.7 eV. Apart from the peculiar case of the Ge_5H_{12} cluster, the correction to the Kohn−Sham gap is larger for the clusters with a smaller diameter in both ΔSCF-LDA and GW approaches. As a result, the quantum-size effect is enhanced with respect to the LDA Kohn−Sham level of description. Such enhancement can be understood in terms of image-potential effects: these push up (down) empty (filled) states close to the cluster boundary, leading to an increase of the gap in small nanoclusters.[13]

For the three largest clusters the GW gaps are larger than the ΔSCF-LDA ones; however, the smallest cluster under study, Ge_5H_{12}, reveals an atypical behavior: the GW gap is smaller than the ΔSCF-LDA one. Indeed, the ΔSCF calculation for such a small cluster is particularly cumbersome because the electron added to the system to obtain the total energy E^{tot}_{N+1} of the negatively charged cluster is not bound in LDA. This implies that its wave function has a very large spatial extent, which makes it hard to converge the calculation. As expected, looking at the square modulus of the wave function of the state that becomes the GW-LUMO in Figure 2a, we see that the largest part of the state is localized away from the cluster.

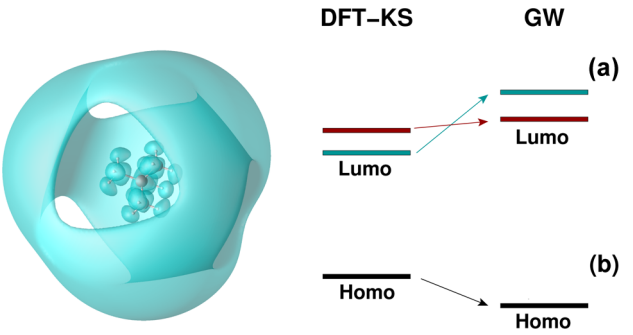

Figure 2. (a) Square modulus of the Kohn−Sham single-particle wave function of the state LUMO+8 of Ge_5H_{12}. The plotted surface is the set of points where the charge density is at the 10% of its maximum value. (b) Schematic representation of the effect of the GW corrections on the ordering of the KS-levels. The GW LUMO was the LUMO+8 in DFT-KS.

Actually, the GW corrections change the character of the LUMO, which at the DFT level is a state localized close to the cluster. This is schematically shown in Figure 2b: within GW calculations, while the Kohn−Sham LUMO of the Ge_5H_{12} dot is pushed high in energy, the LUMO+8 state becomes the new GW quasiparticle LUMO since it is almost not affected by GW self-energy corrections. In numbers: the Kohn−Sham LUMO +8 state, which lies close to the vacuum level, is shifted upward by 0.2 eV while the Kohn−Sham LUMO is shifted upward by as much as 2.5 eV.

This unexpected behavior of the Ge_5H_{12} cluster made us look for differences and analogies in the, in-principle, similar case of hydrogenated Si dots, for which a similar effect had not been reported.[4] After relaxing the structures, we calculated the ΔSCF-LDA and GW gaps of Si_5H_{12}, $Si_{10}H_{16}$, $Si_{35}H_{36}$, and $Si_{87}H_{76}$. The results are listed in Table 3. In contrast with previous results,[4] we find that Si_5H_{12} has the same behavior as Ge_5H_{12}: the GW gap is smaller than the ΔSCF-LDA one, the GW corrections change the character of the LUMO which corresponds to the KS LUMO+14 state, and the new LUMO is mainly localized at a distance from the cluster, just like the GW-LUMO of the Ge_5H_{12} cluster.

Also in the case of Si dots, a qualitative description of the quantum size-effects can be obtained at the LDA Kohn−Sham level, where the Kohn−Sham gap increases from 2.6 to 5.7 eV in agreement with previous calculations.[21] The $Si_{10}H_{16}$ and $Si_{35}H_{36}$ ΔSCF gaps are about 0.6 eV larger than the corresponding gaps calculated in ref 4 (the values in parentheses in Table 3). A similar overestimation of the gap (0.6 and 0.9 eV, respectively) can be found for the GW results. The slightly larger discrepancy of the GW calculations can be addressed to the different GW scheme used in ref 4 where a full TDLDA screening, and the off-diagonal terms of the self-energy operator in the KS basis are taken into account. For the Si_5H_{12} dot, the distance in energy between the GW-corrected KS-LUMO and the GW-HOMO is 9.9 eV, that is 0.5 eV smaller than value reported in ref 4 for the gap of this system. This lies

dx.doi.org/10.1021/jp3121269 | J. Phys. Chem. C XXXX, XXX, XXX−XXX

Table 3. Quasiparticle Gaps Calculated within the ΔSCF-LDA and the GW Methods for Si Clusters of Increasing Diameter[a]

cluster	diameter (nm)	DFT (eV)	ΔSCF-LDA (eV)	GW (eV)	GW-(ΔSCF-LDA) (eV)	GW-DFT (eV)
Si_5H_{12}	0.58	5.7	9.3 (9.2)	8.9 (10.4)	−0.4 (0.94)	3.2
$Si_{10}H_{16}$	0.73	4.6	8.1 (8.7)	8.6[32] (9.2)	0.5 (0.52)	4.0
$Si_{35}H_{36}$	1.10	3.4	5.8 (6.4)	6.2 (7.1)	0.4 (0.7)	2.8
$Si_{87}H_{76}$	1.49	2.6	4.4	5.1	0.7	2.5

[a]The results from ref 4 are in parentheses.

within the range of variation found for the other dots and for the ΔSCF calculations.

According to Tables 2 and 3, we can see that the gaps of Si and Ge dots are similar when their diameters are comparable. A possible crossing of the HOMO−LUMO gaps of clusters of the two materials when the diameter is reduced has been debated. Indeed, a crossing is predicted within the effective mass approximation theory, taking into account the different effective masses of the holes and electrons in bulk Ge and Si.[22] However, previous theoretical works (see ref 8 and references therein) do not show evidence of such crossing. Our calculations confirm the conclusions of these works. The deviation from the effective mass approximation might be explained by the nonparabolicity of the bands, and by the fact that the bulk values of the effective masses for the holes and electrons are not transferable to small clusters, due to the band-folding and mixing of states. In our case only the $Ge_{35}H_{36}$ cluster has a larger gap than the corresponding Si dot. This behavior can be understood in terms of the combination of three different effects: (i) the GW corrections to the DFT gaps (last columns of Tables 3 and 2) follow nicely the dependence on the nanocrystals diameter, i.e., larger corrections for smaller size; (ii) the starting LDA energy gaps are quite similar for Ge and Si nanocrystals with the same number of atoms, a consequence of the much larger Bohr radius of bulk Ge (24.3 nm) with respect to bulk Si (4.9 nm), i.e., the quantum confinement effect is stronger for Ge than for Si; and (iii) Si-bulk has a larger DFT-KS gap than Ge-bulk and comparable GW corrections.[23] Starting from a slightly smaller DFT-KS gap, and having a slightly smaller GW correction, the $Si_{35}H_{36}$ cluster ends up having a smaller GW gap than its Ge counterpart. In contrast, $Si_{10}H_{16}$ has a slightly smaller gap at the DFT-KS level as well, but a larger GW correction ending up with a slightly larger gap than $Ge_{10}H_{16}$.

DISCUSSION

In Figure 3 we compare our ΔSCF-LDA and GW results with previous calculations and experiments for the Ge dots under study. The electronic gap of Ge nanocrystals was measured[6,7] through the analysis of I−V curves of scanning tunneling spectroscopy (STS) measurement (squares and crosses in Figure 3). The theoretical ΔSCF points, as calculated by Melnikov et al.,[8] agree well with our ΔSCF-LDA calculations for both Ge and Si nanoparticles. Apart from the smallest clusters, the GW gaps are systematically larger than the ΔSCF ones, the difference being larger for increasing dot sizes. The extrapolation to lower diameters of the experimental results of ref 6 (using the function $E_g = a_1 + a_2 d^{(-a_3)}$, where E_g is the QP gap, and d is the dot diameter) is in agreement with the GW points (full circles in Figure 3), while the curve obtained from the experimental data set of ref 7 is not in agreement with either theoretical result.

Reference 6 (squares in Figure 3) reported a strong quantum-confinement effect in Ge quantum dots, with an electronic gap that goes from 0.7 eV for a 85 nm dot to 1.8 eV

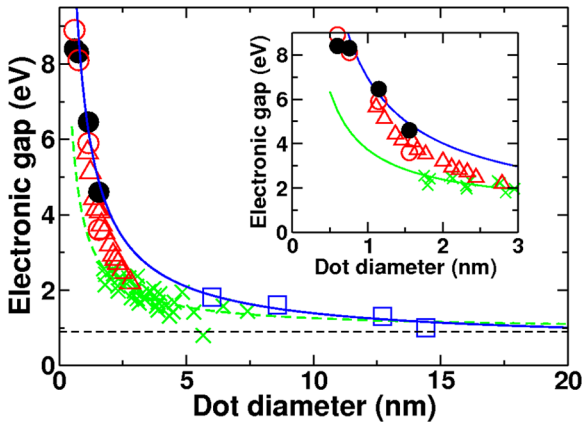

Figure 3. Scaling of the energy gap of Ge nanocrystals with respect to their diameter. Open symbols represent ΔSCF results, while filled symbols are the GW values of the quasiparticle gap; crosses and squares are experimental results. Blue squares: experimental STS results from ref 6; green crosses: experimental STS results from ref 7; red open triangles: theoretical ΔSCF result from ref 8; red open circles: ΔSCF-LDA results; black filled circles: GW results. The solid blue (dashed green) lines correspond to the fitting of the experimental points of ref 6 (ref 7) to the function $E_g = a_1 + a_2 d^{(-a_3)}$ (see the text). The black horizontal dashed line is the Ge bulk band gap value. Inset: Zoom of the graph at low diameters.

for a 5 nm dot. In ref 7 (crosses in Figure 3) the quantum-confinement effect is weaker. The difference between the two experimental data sets can be addressed to the different type of growth. Both experiments were carried out on Ge-dots grown on Si/SiO_2 substrate, but the quantum dots of Nakamura et al.[7] were grown, epitaxially, at high temperature, on the Si substrate to which the dots were connected through ultrasmall voids in the SiO_2 film. In ref 24 it was shown that, for SiGe nanowires, the quantum-confinement effect is reduced in the presence of a Si/Ge interface. The epitaxial growth of the Ge-dots directly on the Si substrate, through the voids of the SiO_2 layer, leads to a Si/Ge interface, and can thus explain the reduced quantum-confinement of the data presented in ref 7.

In Figure 3, the full and dashed lines are the result of the fit of the experimental data to the function $E_g = a_1 + a_2 d^{(-a_3)}$, where E_g is the QP gap, and d is the dot diameter. The effective mass approximation[25] predicts a $1/d^2$ behavior of the electronic gap with respect to the cluster size. However, the scaling extracted from experimental data is typically slower than $1/d^2$, mainly because of the non truly parabolic character of the bands and of screening effects.[26] Also in our case, $a_3 = 0.89$ for the experimental points from ref 6 and $a_3 = 0.95$ for the ones of ref 7. In principle, the a_1 parameter should be equal to the bulk minimum band gap (dashed line in Figure 3). However, fitting ref 7 experimental points, we obtain $a_1 = 0.95$ eV, higher than the value of the Ge bulk band gap. It is shown that the gap of bulk Si/Ge alloys increases with its Si content.[27] The high value of a_1 for ref 7 experimental points can thus be explained by the

dx.doi.org/10.1021/jp3121269 | J. Phys. Chem. C XXXX, XXX, XXX−XXX

presence of Si/Ge alloy at the Si/Ge interface (such interface is not present in the case of ref 6 for which the fit gives a_1 = 0.56 eV).

Besides the case of the smallest nanoparticles, we find that ΔSCF-LDA gaps are always smaller than GW ones (see Table 2). The difference between the results of the two methods increases with the diameter for the Ge systems while this growth is less evident for the Si ones. Apart from the smallest dots, such findings are in agreement with theoretical calculations concerning the IP and the EA of hydrogenated Si dots of ref 4. Altogether these results suggest that the picture of ref 13 is oversimplified. In ref 13 it was in fact suggested that for 0-D systems the missing contribution in the ΔSCF-LDA approach Δ is approximately given by the bulk self-energy term, namely $\Delta \approx \Delta_b$. In Figure 4 $\Delta - \Delta_b$, as given by eq 9 in ref 13,

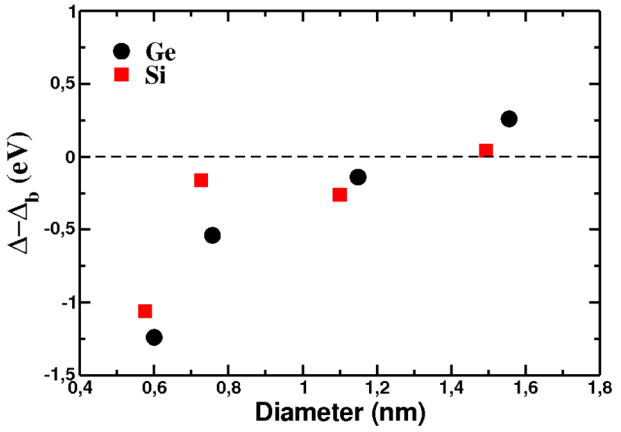

Figure 4. $\Delta - \Delta_b$ as given from eq 9 of ref 13 for the clusters under study as a function of diameter. Red squares: Si dots; black circles: Ge dots.

is plotted as a function of the dot diameter for both the Si and Ge dots. Clearly $\Delta - \Delta_b$ deviates from zero and is negative for the smaller clusters and positive for the largest clusters under study. Moreover, we see in Table 2 that the deviation of the ΔSCF-LDA results from the GW ones exceeds the Ge bulk self-energy correction ($\Delta_b \approx 0.5$ eV) in case of the Ge nanocrystal with a diameter ≤1.6 nm. The GW approximation embodies, unlike ΔSCF-LDA, dynamical effects and, more importantly, a nonlocal exchange potential. Nonlocal exchange is more efficient in opening the gap than local exchange, so it might be expected that GW gaps are consistently larger than ΔSCF-LDA gaps. Indeed this happens for most of the cases. However, ΔSCF-LDA results cannot be thought of as lower bound values of the QP gaps: in the case of the smallest clusters under study and of the small Ag clusters studied in ref 5, the GW gaps are smaller than ΔSCF-LDA ones. In the case of the semiconductor clusters the reason for this behavior can be found in the delocalized nature of the conduction band minimum. Such nature, typical of Rydberg states, determines a completely different effect in the self-energy shift of the single-electron energy level, which is 1 order of magnitude lower with respect to the quasiparticle shift of the other conduction states. In principle, Rydberg states should be bound states. However, the LDA potential is not able to describe them correctly due to its long-range exponential decay. As a consequence, image states result often unbound at the DFT-LDA level. In such cases, the LDA Kohn−Sham wave function is likely a bad approximation to the quasiparticle one, and a full diagonalization of the quasiparticle Hamiltonian would be required.[28] This is what happens for the LiF(001)-(1 × 1) surface[29] and jellium clusters.[30] For these systems the determination of the quasiparticle wave function beyond DFT-LDA was needed. Moreover a recent calculation on small hydrogenated carbon clusters[31] using time-dependent density functional theory (TDDFT) shows that a better agreement with experiments is achieved when Rydberg states are treated more accurately by using hybrid functionals. Interestingly, in ref 31 the poor description of Rydberg states was responsible for a too large gap in the TDDFT spectra within the adiabatic LDA approximation. All these facts suggest that also for our smallest clusters the gaps obtained within ΔSCF-LDA are larger than the GW ones due to the wrong asymptotics of the LDA xc potential.

CONCLUSIONS

In conclusion we have computed the quasiparticle gaps of hydrogenated Ge nanocrystals of increasing size within the GW approximation and the ΔSCF-LDA methods comparing them with the best known nanosystems based on Si.

Although both methods give large corrections with respect to Kohn−Sham gaps, we find that the two approaches are not equivalent. The difference between the two methods increases when the dot diameter increases, but it does not follow a smooth predictable trend. In general, the GW gaps are larger with respect to the ΔSCF-LDA ones; however, the smallest cluster shows an atypical behavior, related to the Rydberg character of its LUMO which is badly described by using the LDA. We found a similar behavior also in the case of Si_5H_{12}. Due to a poor description of Rydberg states within LDA, more sophisticated calculations, including, for instance, the diagonalization of the quasiparticle Hamilonian or the use of hybrid functionals, are envisaged for a quantitative determination of the HOMO−LUMO gap. Finally, we have shown that deviation of the ΔSCF-LDA results from the GW ones can clearly exceed the bulk self-energy correction.

AUTHOR INFORMATION

Corresponding Author

*E-mail: margherita.marsili@pd.infn.it.

Notes

The authors declare no competing financial interest.

ACKNOWLEDGMENTS

We are grateful for discussions with M. De Crescenzi, P. Castrucci, and M. Scarselli. The research leading to these results has received funding from the European Community's Seventh Framework Programme (FP7/2007-2013) under grant agreements no. 211956 (ETSF project no. 48) and no. 246937 (IRSES SIMTECH) and by MIUR-PRIN 2007. Computer resources from INFM Progetto Calcolo Parallelo at CINECA, and CASPUR are gratefully acknowledged. We also acknowledge ENEA and its HPC team for supporting our computational activities on the ENEA-GRID (CRESCO) infrastructure (www.cresco.enea.it). Some of the calculations were performed at the LCA of the University of Coimbra and at IDRIS (project x2010096017, projet GENCI 544). S.B. acknowledges financial support from the Programme PIR Materiaux-MaProSu of CNRS. M.A.L.M. acknowledges partial support from the Portuguese FCT through the project PTDC/FIS/73578/2006 and from the French ANR (ANR-08-CEXC8-008-01).

REFERENCES

(1) Jones, R. O.; Gunnarsson, O. The Density Functional Formalism, its Applications and Prospects. *Rev. Mod. Phys.* **1989**, *61*, 689−746.
(2) Hedin, L.; Lundqvist, S. Effects of Electron-Electron and Electron-Phonon Interactions on the One-Electron States of Solids. *Solid State Physics* **1969**, *23*, 1−181.
(3) Aulbur, W. G.; Jönsson, L.; Wilkins, J. W. Quasiparticle Calculations in Solids. *Solid State Phys.* **2000**, *54*, 1−218.
(4) Tiago, M. L.; Chelikowsky, J. R. Optical Excitations in Organic Molecules, Clusters, and Defects Studied by First-Principles Green's Function Methods. *Phys. Rev. B* **2006**, *73*, 205334−205352.
(5) Tiago, M. L.; Idrobo, J. C.; Öğüt, S.; Jellinek, J.; Chelikowsky, J. R. Electronic and Optical Excitations in Ag_n Clusters (n=1−8): Comparison of Density-Functional and Many-Body Theories. *Phys. Rev. B* **2009**, *79*, 155419−155432.
(6) Scarselli, M.; Masala, S.; Castrucci, P.; De Crescenzi, M.; Gatto, E.; Venanzi, M.; Karmous, A.; Szkutnik, P. D.; Ronda, A.; Berbezier, I. Optoelectronic Properties in Quantum-Confined Germanium Dots. *Appl. Phys. Lett.* **2007**, *91*, 141117−141119.
(7) Nakamura, Y.; Watanabe, K.; Fukuzawa, Y.; Ichikawa, M. Observation of the Quantum-Confinement Effect in Individual Ge Nanocrystals on Oxidized Si Substrates Using Scanning Tunneling Spectroscopy. *Appl. Phys. Lett.* **2005**, *87*, 133119−133122.
(8) Melnikov, D. V.; Chelikowsky, J. R. Electron Affinities and Ionization Energies in Si and Ge Nanocrystals. *Phys. Rev. B* **2004**, *69*, 113305−113308.
(9) Godby, R. W.; Schlüter, M.; Sham, L. J. Accurate Exchange-Correlation Potential for Silicon and Its Discontinuity on Addition of an Electron. *Phys. Rev. Lett.* **1986**, 2415−2418.
(10) Grüning, M.; Marini, A.; Rubio, A. Density Functionals from Many-Body Perturbation Theory: The Band Gap for Semiconductors and Insulators. *J. Chem. Phys.* **2006**, *124*, 154108−154116.
(11) Grüning, M.; Marini, A.; Rubio, A. Effect of Spatial Nonlocality on the Density Functional Band Gap. *Phys. Rev. B* **2006**, *74*, 161103−161106(R).
(12) Seidl, A.; Görling, A.; Vogl, P.; Majewski, J. A.; Levy, M. Generalized Kohn-Sham Schemes and the Band-Gap Problem. *Phys. Rev. B* **1996**, *53*, 3764−3774.
(13) Delerue, C.; Allan, G.; Lannoo, M. Dimensionality-Dependent Self-Energy Corrections and Exchange-Correlation Potential in Semiconductor Nanostructures. *Phys. Rev. Lett.* **2003**, *90*, 076803−076806.
(14) Giannozzi, P.; Baroni, S.; Bonini, N.; Calandra, M.; Car, R.; Cavazzoni, C.; Ceresoli, D.; Chiarotti, G. L.; M. Cococcioni, M.; Dabo, I.; et al. QUANTUM ESPRESSO: a Modular and Open-Source Software Project for Quantum Simulations of Materials. *J. Phys.: Condens. Matter* **2009**, *21*, 395502.
(15) Weissker, H.-C.; Ning, N.; Bechstedt, F.; Vach, H. Luminescence and Absorption in Germanium and Silicon Nanocrystals: The Influence of Compression, Surface Reconstruction, Optical Excitation, and Spin-Orbit Splitting. *Phys. Rev. B* **2011**, *83*, 125413−125418.
(16) Marini, A.; Hogan, C.; Grüning, M.; Varsano, D. Yambo: An Ab Initio Tool for Excited State Calculations. *Comput. Phys. Commun.* **2009**, *180*, 1392−1403.
(17) Onida, G.; Reining, L.; Godby, R. W.; Del Sole, R.; W. Andreoni, W. Ab Initio Calculations of the Quasiparticle and Absorption Spectra of Clusters: The Sodium Tetramer. *Phys. Rev. Lett.* **1995**, *75*, 818−821.
(18) The ΔSCF calculations have been performed using the code OCTOPUS: Castro, A.; Appel, H.; Oliveira, M.; Rozzi, C. A.; Andrade, X.; Lorenzen, F.; Marques, M. A. L.; Gross, E. K. U.; Rubio, A. Octopus: a Tool for the Application of Time-Dependent Density Functional Theory. *Phys. Status Solidi B* **2006**, *243*, 2465−2488. Marques, M. A. L.; A. Castro, A.; Bertsch, G. F.; Rubio, A. Octopus: a First-Principles Tool for Excited Electron-Ion Dynamics. *Comput. Phys. Commun.* **2003**, *151*, 60−78.
(19) Perdew, J. P.; Zunger, A. Self-Interaction Correction to Density-Functional Approximations for Many-Electron Systems. *Phys. Rev. B* **1981**, *23*, 5048−5079.
(20) Troullier, N.; Martins, J. L. Efficient Pseudopotentials for Plane-Wave Calculations. *Phys. Rev. B* **1991**, *43*, 1993−2006.
(21) Degoli, E.; Cantele, G.; Luppi, E.; Magri, R.; Ninno, D.; Bisi, O.; Ossicini, S. Ab Initio Structural and Electronic Properties of Hydrogenated Silicon Nanoclusters in the Ground and Excited State. *Phys. Rev. B* **2004**, *69*, 155411−155420.
(22) Takagahara, T.; Takeda, K. Theory of the Quantum Confinement Effect on Excitons in Quantum Dots of Indirect-Gap Materials. *Phys. Rev. B* **1992**, *46*, 15578−15581(R).
(23) Hybertsen, M. S.; Louie, S. G. Electron Correlation in Semiconductors and Insulators: Band Gaps and Quasiparticle Energies. *Phys. Rev. B* **1986**, *34*, 5390−5413.
(24) Amato, M.; Palummo, M.; Ossicini, S. Reduced Quantum Confinement Effect and Electron-Hole Separation in SiGe Nanowires. *Phys. Rev. B* **2009**, *79*, 201302−201305(R).
(25) Brus, L. E. A Simple Model for the Ionization Potential, Electron Affinity, and Aqueous Redox Potentials of Small Semiconductor Crystallites. *J. Chem. Phys.* **1983**, *79*, 5566−5571.
(26) Franceschetti, A.; Zunger, A. Direct Pseudopotential Calculation of Exciton Coulomb and Exchange Energies in Semiconductor Quantum Dots. *Phys. Rev. Lett.* **1997**, *78*, 915−918.
(27) Braunstein, R.; Moore, A. R.; Herman, F. Intrinsic Optical Absorption in Germanium-Silicon Alloys. *Phys. Rev.* **1958**, *109*, 695−710.
(28) Pulci, O.; Bechstedt, F.; Onida, G.; Del Sole, R.; Reining, L. State Mixing for Quasiparticles at Surfaces: Nonperturbative GW Approximation. *Phys. Rev. B* **1999**, *60*, 16758−16761.
(29) Rohlfing, M.; Wang, N.-P.; Krüger, P.; Pollmann, J. Image States and Excitons at Insulator Surfaces with Negative Electron Affinity. *Phys. Rev. Lett.* **2003**, *91*, 256802−256805.
(30) Rinke, P.; Delaney, K.; García-González, P.; Godby, R. W. Image States in Metal Clusters. *Phys. Rev. A* **2004**, *70*, 063201−063205.
(31) Vörös, M. A.; Gali, A. Optical Absorption of Diamond Nanocrystals From Ab Initio Density-Functional Calculations. *Phys. Rev. B* **2009**, *80*, 161411−161414(R).
(32) Luppi, E.; Iori, F.; Magri, R.; Pulci, O.; Ossicini, S.; Degoli, E.; Olevano, V. Excitons in Silicon Nanocrystallites: The Nature of Luminescence. *Phys. Rev. B* **2007**, *75*, 033303−033306.